VSV Oncolysis in Combination With the BCL-2 Inhibitor Obatoclax Overcomes Apoptosis Resistance in Chronic Lymphocytic Leukemia

Sara Samuel[1,2], Vanessa F Tumilasci[1,2], Stephanie Oliere[1,2], Thi Liên-Anh Nguyên[1], April Shamy[3], John Bell[4] and John Hiscott[1–3]

[1]Molecular Oncology Group, Lady Davis Institute for Medical Research, Jewish General Hospital, Montreal, Quebec, Canada; [2]Department of Microbiology and Immunology, McGill University, Montreal, Quebec, Canada; [3]Department of Medicine, Jewish General Hospital, McGill University, Montreal, Quebec, Canada; [4]Ottawa Health Research Institute, University of Ottawa, Ottawa, Ontario, Canada

In chronic lymphocytic leukemia (CLL), overexpression of antiapoptotic B-cell leukemia/lymphoma 2 (BCL-2) family members contributes to leukemogenesis by interfering with apoptosis; BCL-2 expression also impairs vesicular stomatitis virus (VSV)-mediated oncolysis of primary CLL cells. In the effort to reverse resistance to VSV-mediated oncolysis, we combined VSV with obatoclax (GX15-070)—a small-molecule BCL-2 inhibitor currently in phase 2 clinical trials—and examined the molecular mechanisms governing the *in vitro* and *in vivo* antitumor efficiency of combining the two agents. In combination with VSV, obatoclax synergistically induced cell death in primary CLL samples and reduced tumor growth in severe combined immunodeficient (SCID) mice-bearing A20 lymphoma tumors. Mechanistically, the combination stimulated the mitochondrial apoptotic pathway, as reflected by caspase-3 and -9 cleavage, cytochrome c release and BAX translocation. Combination treatment triggered the release of BAX from BCL-2 and myeloid cell leukemia-1 (MCL-1) from BAK, whereas VSV infection induced NOXA expression and increased the formation of a novel BAX-NOXA heterodimer. Finally, NOXA was identified as an important inducer of VSV-obatoclax driven apoptosis via knockdown and overexpression of NOXA. These studies offer insight into the synergy between small-molecule BCL-2 inhibitors such as obatoclax and VSV as a combination strategy to overcome apoptosis resistance in CLL.

INTRODUCTION

Chronic lymphocytic leukemia (CLL) is caused by a defect in apoptosis rather than increased proliferation of CD5^{+} B lymphocytes.[1,2] Resistance to cytotoxic treatments in CLL is largely due to the overexpression of antiapoptotic B-cell lymphoma-2 (BCL-2) family members BCL-2 and myeloid cell leukemia (MCL-1).[3,4] High levels of BCL-2 in CLL patients correlates to decreased overall survival and chemoresistance, whereas MCL-1 overexpression is associated with failure to achieve complete remission.[5–7] BCL-2 proteins are subdivided into anti- and proapoptotic classes. Prosurvival members such as BCL-2, BCL-xL, A1, and MCL-1 block apoptosis by binding to and preventing proapoptotic members such as BAX and BAK from oligomerizing and forming pores at the mitochondrial membrane that trigger mitochondrial depolarization.[8–10] BH-3-only proteins (BIM, tBID, PUMA, NOXA, BAD) bind to antiapoptotic members of the BCL-2 family (MCL-1, BCL-2, BCL-x_L, BCL-w), resulting in the release of proapoptotic BAX and/or BAK[9,11] or directly bind and activate BAX/BAK.[8]

Knowledge that overexpression of BCL-2 proteins leads to resistance in many cancers has sparked considerable interest in the development of small-molecule BCL-2 inhibitors.[12,13] Encouraging results with BCL-2 inhibitors—either alone or in combination with standard chemotherapies—have been demonstrated with various cancers, including CLL.[13–15] obatoclax (GX15-070)—one of the promising pan-BCL-2 inhibitors currently in clinical trials—is an indole-derived broad-spectrum inhibitor with multiple targets among the BCL-2 proteins. Obatoclax binds to the hydrophobic pocket within the BH-3-binding groove of antiapoptotic proteins such as BCL-2, MCL-1, and BCL-xL, and interferes with the ability of these proteins to interact with and negatively regulate proapoptotic BCL-2 proteins such as BAX and BAK.[16,17] In preclinical studies, obatoclax has shown cytotoxic efficacy against a variety of cancers including myeloma, breast cancer, mantle cell lymphoma, and nonsmall cell lung cancer cells.[16,18–20]

Oncolytic viruses have emerged as a potential treatment for solid tumors and hematological malignancies.[21–23] By exploiting tumor-specific defects in the interferon signaling pathway, vesicular stomatitis virus (VSV)—a prototypical oncolytic virus—infects and replicates specifically within cancerous cells, resulting in apoptotic cell death. Initiation of apoptosis by VSV can occur through the intrinsic mitochondrial pathway, via induction of

the BH-3-only, proapoptotic protein NOXA,[25–27] or through the extrinsic pathway via caspase-8 and BID cleavage.[28,29]

We previously showed that the resistance of CLL cells to VSV-induced oncolysis can be overcome using a combination of VSV with small-molecule BCL-2 inhibitors.[23] In the present study, we used the pan-BCL-2 family inhibitor obatoclax and characterized the mechanism governing its synergistic effect with VSV. Combination therapy triggered intrinsic apoptosis leading to caspase-9 and -3 activation, BAX translocation and cytochrome c release. The efficacy of the VSV-obatoclax combination was further demonstrated *in vivo* where reduced tumor progression in an A20 murine B-lymphoma xenograft model was observed. The proapoptotic protein NOXA was identified as a central inducer of apoptosis that increased the ratio of proapoptotic BAX and BAK containing complexes at the mitochondrial membrane.

RESULTS

VSV-obatoclax combination synergistically induces cell death in primary CLL cells

To determine the lowest efficient dose of obatoclax that could be used in combination with VSV, a dose-dependent killing curve was performed in primary $CD5^+$ $CD19^+$ CLL cells (**Figure 1a**). Obatoclax had an IC_{50} of 640 nmol/l, lower than the IC_{50} (1 µmol/l) in peripheral blood mononuclear cells (PBMCs) from healthy volunteers; however at 640 nmol/l, obatoclax killed a significant amount (30%) of healthy PBMCs (**Figure 1a**). A lower dose of 100 nmol/l of obatoclax was sufficient to synergistically trigger cell death in 72% ($P < 0.001$) of primary $CD5^+$ $CD19^+$ CLL samples infected with VSV (10 multiplicity of infection), but did not induce >8% cell death in healthy PBMCs. Each treatment alone showed minimal killing activity in primary CLL cells (5 and 25% for VSV and obatoclax, respectively (**Figure 1b**)). The enhanced cytotoxic effect of VSV-obatoclax was not prominent with obatoclax doses <100 nmol/l. These results demonstrate synergistic cytotoxicity of $CD5^+$ $CD19^+$ CLL cells using the VSV-obatoclax, combination, with minimal cytotoxic effect on healthy PBMCs at 100 nmol/l obatoclax.

BCL-2 inhibits apoptosis by binding BAX, thus preventing mitochondrial pore formation and membrane permeabilization.[9–11] To determine the effect of obatoclax on BCL-2–BAX interaction, anti-BAX coimmunoprecipitations were performed in Karpas-422 cells, treated with increasing doses of inhibitor (0—1,000 nmol/l). Obatoclax inhibited the interaction between BCL-2 and BAX at high concentrations (>500 nmol/l), whereas at 100 nmol/l no disruption of BCL-2/BAX was observed (**Figure 1c**), thus demonstrating that 100 nmol/l obatoclax was suboptimal as a single treatment.

Obatoclax increases VSV-induced oncolysis in A20 B-lymphoma xenograft tumors in SCID mice

After establishing the cytotoxicity of combination therapy on CLL cells *in vitro*, the antitumor effects of VSV-obatoclax were examined *in vivo* in Fox Chase severe combined immunodeficient (SCID) mice-bearing A20 xenograft tumors. Like Karpas-422 and primary CLL cells, A20 B-lymphoma cells overexpress BCL-2 (**Figure 2a**) and are partially resistant to VSV-induced apoptosis. *In vitro*, obatoclax treatment of A20 cells decreased viability by 10%, whereas VSV infection resulted in a 40% decrease; the
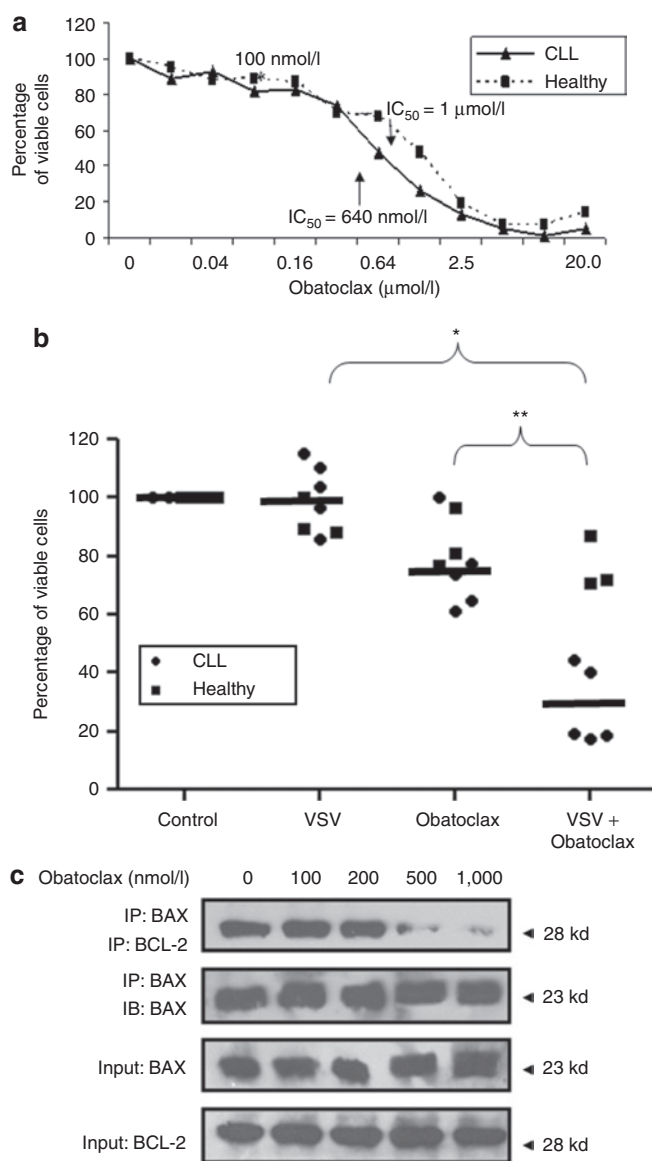

Figure 1 VSV-obatoclax combination therapy enhances cytotoxicity in $CD5^+$ $CD19^+$ CLL cells. (a) The IC_{50} of obatoclax was determined in PBMCs from CLL patients and healthy volunteers; PBMCs were treated with varying concentrations of obatoclax (0–20 µmol/l) and cell viability was assessed by MTT assay. The results are reported as percentage of viable cells; values represent the mean of quadruplicate experiments ± SD. **(b)** Cell viability of PBMCs from five CLL patients and four healthy volunteers was assessed by MTT assay. The results are reported on a scatter graph as percentage of viable cells (*$P < 0.01$; **$P < 0.0001$); the mean value for all patients within a group is indicated by the line. **(c)** Karpas-422 cells were treated with different concentrations of obatoclax (100–1,000 nmol/l) for 24 hours. Cells were lysed in 1% CHAPS lysis buffer and BAX was immunoprecipitated (IP) followed by immunoblotting (IB) with anti-BCL-2 antibody. BCL, B-cell lymphoma-2; CLL, chronic lymphocytic leukemia; PBMC, peripheral blood mononuclear cell; VSV, vesicular stomatitis virus.

combination reduced viability by 70% (**Figure 2b**). To determine the effect of the combination *in vivo*, SCID mice were injected with 1×10^6 A20 cells; when tumors were palpable at day 12, animals received obatoclax 3 mg/kg/day (intraperitoneal injection) for five consecutive days (days 12–16) and two intratumoral injections of
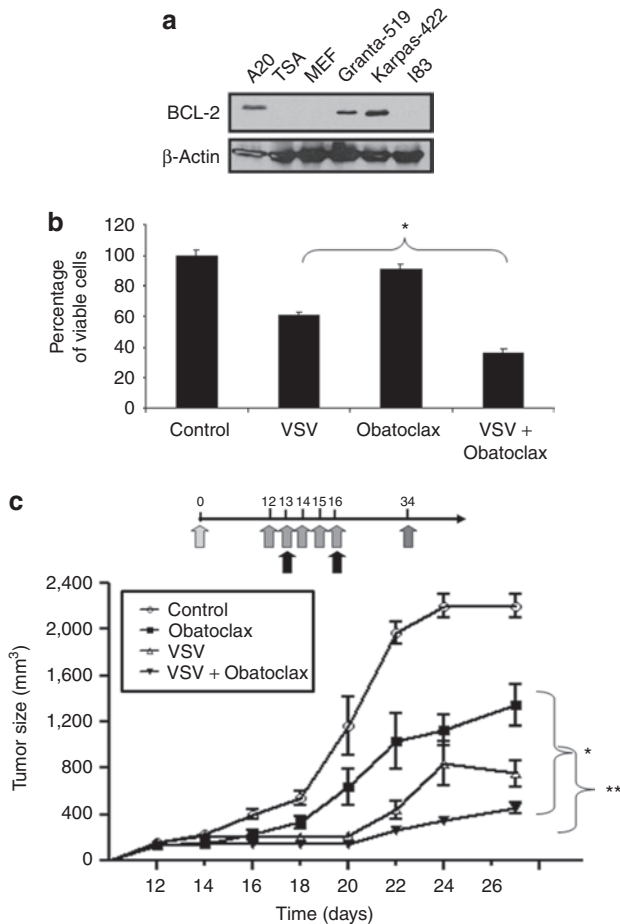
Figure 2 Obatoclax treatment augments VSV-mediated oncolysis in A20 B-lymphoma xenografts in SCID mice. (a) BCL-2 expression. Proteins from six different B-lymphoma cell lines were isolated using 1% CHAPS buffer. BCL-2 expression in A20 cells compared to Grantas-519 and Karpas-422 cells was analyzed by western blot with anti-BCL-2 antibody. **(b)** Viability of A20. Cells were treated with or without VSV and obatoclax. At 72 hours postinfection, cell viability was assessed by MTT assay. Results are reported as percentage of viable cells ± SD; each experiment was performed in quadruplicate (*$P < 0.01$). **(c)** A20 murine B-lymphoma cells were inoculated into the flank of SCID mice on day 0. Mice-bearing A20 xenograft tumors received five intraperitoneal injections of obatoclax and two intratumoral VSV injections, beginning on day 12, through day 16. The stars indicate $P < 0.001$ comparing tumor size between the single and combination treatment groups. Tumor volumes were calculated as ½(length × width^2) and values are expressed as the mean ± SD of tumor volume ($n = 8$). BCL, B-cell lymphoma-2; CLL, chronic lymphocytic leukemia; PBMC, peripheral blood mononuclear cell; SCID, severe combined immunodeficient; VSV, vesicular stomatitis virus.

1×10^8 plaque-forming units of VSV at days 13 and 16 (**Figure 2c**). As shown in **Figure 2c**, tumors grew to a diameter of ~2,200 mm^3 by day 26 without treatment. Treatment with obatoclax led to a 40% decrease in tumor size compared to untreated animals. Mice receiving VSV alone exhibited 65% suppression of tumor growth compared to control animals. Tumor growth was decreased further with the VSV-obatoclax combination (80%).

VSV-obatoclax activates apoptosis through the intrinsic pathway

After establishing the efficacy of the combination therapy *in vitro* and *in vivo*, the mechanism(s) by which the individual and
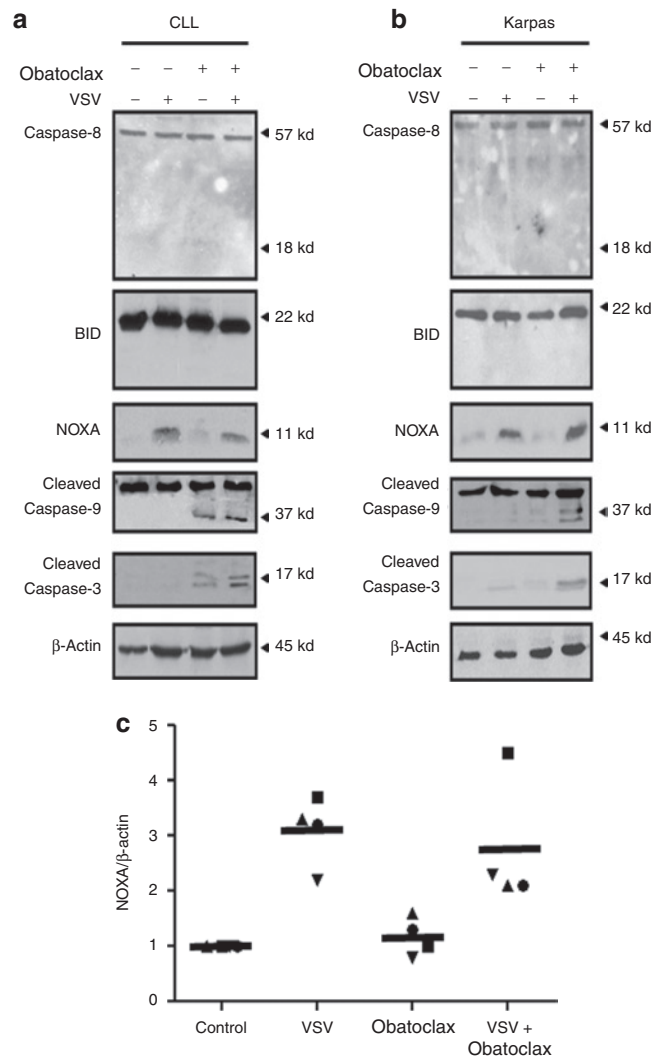

Figure 3 VSV-obatoclax combination activates the intrinsic apoptotic pathway. The effect of VSV and obatoclax single or combination treatments on cleavage of caspase-3, -8, -9 and BID and NOXA expression in **(a)** PBMCs isolated from CLL patients and **(b)** Karpas-422 cells was analyzed by immunoblotting. Cells were lysed in 1% CHAPS lysis buffer. Protein lysates were subjected to immunoblot analysis with antibodies that recognize NOXA, cleaved caspase-3 and both cleaved and uncleaved forms of caspase-8, -9, and BID. The CLL patient blots were performed in $n = 3$ patients and a representative CLL patient is shown. **(c)** Primary PBMCs isolated from CLL patients were pretreated in the presence or absence of VSV-obatoclax. NOXA and β-actin mRNA levels were determined by real-time PCR. The scatter graphic shows level of NOXA mRNA expression in PBMCs from CLL patients; the line demonstrates the mean value for all patients ($n = 4$). CLL, chronic lymphocytic leukemia; PBMC, peripheral blood mononuclear cell; VSV, vesicular stomatitis virus.

combination treatment induced oncolysis was evaluated. Key proteins involved in triggering the extrinsic (caspase 8) and intrinsic (caspase-9) apoptotic pathways were examined, as well as downstream effectors (BID and caspase-3). The amount of cleaved caspase-3 was increased threefold (**Figure 3a**, lane 4) in CLL cells with the combination compared to obatoclax alone and was increased more than fivefold (**Figure 3b**, lane 4) in Karpas-422 cells compared to VSV or obatoclax, whereas caspase-8 and BID cleavage were not detected following single or combination treatments
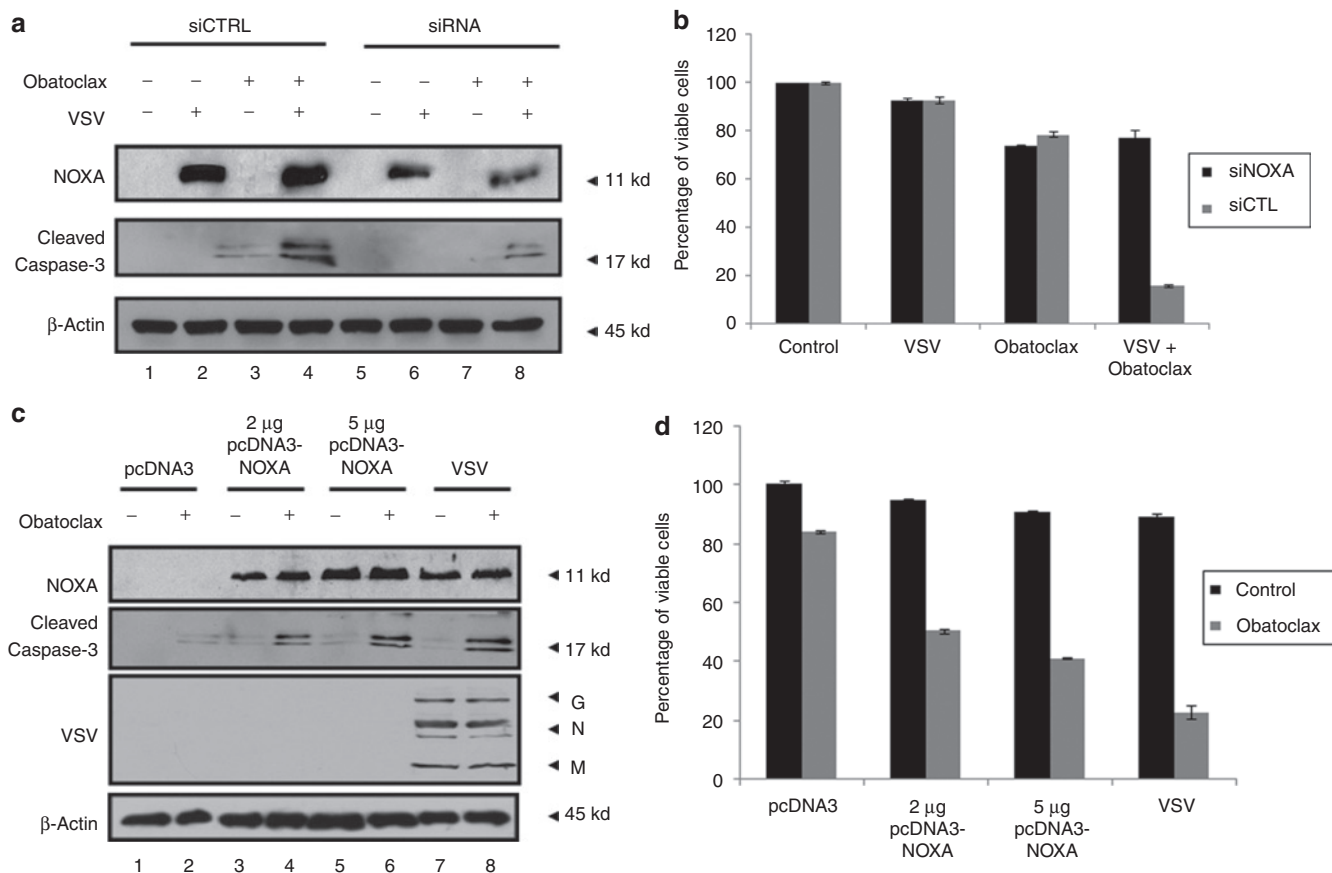
Figure 4 Induction of NOXA expression is necessary and sufficient to synergistically induce apoptosis with obatoclax. (a–b) Karpas-422 B-lymphoma cells were transiently transfected with siRNA targeting human NOXA (siNOXA) or the nontargeting control pool (siControl). At 24 hours post-transfection, cells were treated with obatoclax followed or not by VSV infection. **(a)** At 24 hours postinfection, cells were lysed and NOXA silencing was analyzed by immunoblot using anti-NOXA antibody. Caspase-3 cleavage was also determined using an anti-caspase-3 antibody. **(b)** Cell viability analysis by Annexin V/PI staining was performed on cells treated as described in **a**. Black bars represent Karpas-422 cells treated with siNOXA and gray bars represent cells treated with siControl. The data shown are the mean ± SEM ($n = 3$). **(c–d)** Karpas-422 B-lymphoma cells were transiently transfected with human pcDNA3-NOXA or empty vector. At 24 hours post-treatment, cells were lysed and NOXA expression, caspase-3 cleavage and VSV replication were analyzed by immunoblot. G, glycoprotein; M, matrix; N, nucleocapsid. **(b)** Cell viability was determined by FACS analysis after Annexin V/PI staining. **(d)** Black bars represent nontreated Karpas-422 cells and gray bars represent cells treated with obatoclax. The data shown are the mean ± SEM ($n = 3$). FACS, fluorescence-activated cell sorting; VSV, vesicular stomatitis virus.

(**Figure 3a,b**). Because of the key role for caspase-8 as an initiator of the extrinsic pathway[30] and as an activator of BID cleavage,[31] we concluded that activation of the extrinsic pathway was not involved in VSV-obatoclax induced apoptosis. In contrast, VSV-obatoclax treatment effectively induced caspase-9 cleavage (**Figure 3a,b**, lane 4), the initiator for the intrinsic mitochondrial pathway.[32]

NOXA induction is essential for obatoclax-mediated apoptosis in Karpas-422 cells

Following VSV infection, the BH-3 only proapoptotic protein NOXA is transcriptionally induced in an interferon regulatory factor-3 and p53-dependent manner.[25–27] To determine whether NOXA contributes to VSV-induced apoptosis in CLL, NOXA expression was measured in CLL and Karpas-422 cells. VSV infection alone or in combination with obatoclax-induced NOXA expression equivalently at the RNA and protein levels (**Figure 3a–c**). Whereas VSV infection did not to trigger caspase-3 cleavage (**Figure 3a,b**) or loss of cell viability (**Figure 1b**), the combination resulted in caspase-3

cleavage and decreased cell viability. Silencing of NOXA by introduction of small-interfering RNA (siRNA) resulted in reduced caspase-3 cleavage in cells treated with VSV-obatoclax (**Figure 4a**). Furthermore, siRNA knockdown of NOXA impaired the VSV-obatoclax-induced apoptotic response by 60% in Karpas-422 cells (**Figure 4b**), indicating an important role for VSV-induced NOXA expression in the synergic effect of VSV-obatoclax.

Furthermore, replacing VSV infection by NOXA overexpression demonstrated that the combination of NOXA and obatoclax is able to induce caspase-3 cleavage (**Figure 4c**, lanes 4 and 6) and cell killing (**Figure 4d**) to levels comparable to VSV-obatoclax combination therapy (**Figure 4c**, lanes 8 and **Figure 4d**), suggesting that NOXA is sufficient for induction of apoptosis.

VSV-obatoclax combination triggers BAX translocation and cytochrome c release

To examine further the effect of the VSV-obatoclax combination on the stimulation of the intrinsic apoptotic pathway, BAX

translocation, oligomerization—determined by the detection of the activated form of BAX with the conformation-specific antibody 6A7—cytochrome c release and NOXA expression in the mitochondria were examined. Treatment with VSV or obatoclax
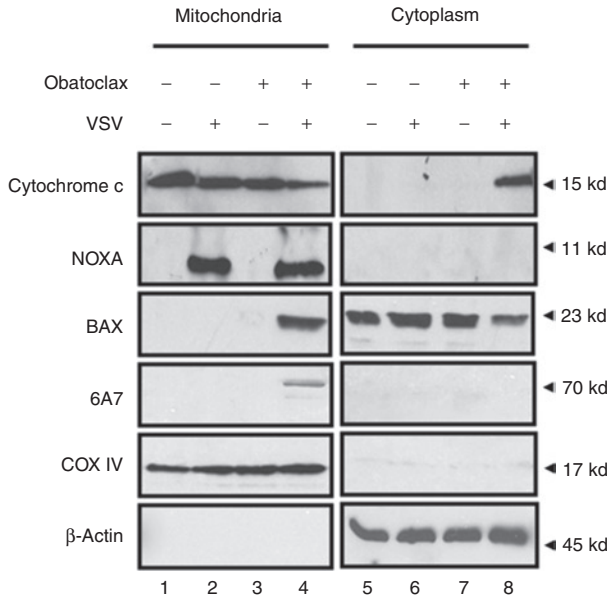

Figure 5 VSV-obatoclax induces BAX translocation to the mitochondria and cytochrome c release into the cytoplasm. Following 24 hours, VSV-obatoclax treatment Karpas-422 cells were harvested and mitochondria were isolated using the Pierce mitochondria isolation kit, reagent-based method. The mitochondria-free cytosolic fraction was analyzed for cytochrome c release by immunoblotting using specific antibodies for cytochrome c. The mitochondrial fraction was analyzed for NOXA expression, BAX 6A7 oligomerization and BAX translocation using anti-NOXA, -6A7 and -BAX antibodies. COX IV and β-actin were used as a loading control for mitochondrial and cytosolic fractions, respectively. VSV, vesicular stomatitis virus.

alone did not induce BAX translocation, activation, or cytochrome c release (**Figure 5**, lanes 2, 3, 6, and 7). VSV-obatoclax combination treatment resulted in recruitment and activation of BAX at the mitochondrial membrane (**Figure 5**, lane 4) and cytochrome c release into the cytoplasm (**Figure 5**, lane 8). NOXA protein expression was induced and localized to the mitochondrial fraction in VSV- and VSV-obatoclax-treated cells (**Figure 5**, lanes 2 and 4). Although VSV alone induced NOXA expression, it was not sufficient to trigger apoptosis and only the VSV-obatoclax combination induced the translocation of activated BAX to the mitochondria and cytochrome c release. Further analysis of BCL-2 family proteins demonstrated that the levels of MCL-1, BAK, and BCL-2 were not altered by VSV or obatoclax single or combination treatments (data not shown).

BCL-2 is overexpressed in primary cells from CLL patients

It was previously shown that overexpression of different BCL-2 family members—predominantly BCL-2 and MCL-1—correlate with poor prognosis, disease progression, and resistance to treatment in CLL patients.[5–7] Immunoblot analysis showed that BCL-2 was overexpressed in PBMCs isolated from CLL patients, compared with PBMCs from healthy volunteers (**Figure 6a**). Karpas-422 and Granta-519 expressed BCL-2 levels similar to those observed in CLL patients, as previously shown,[23] whereas other B-cell lines (L428, CRO) displayed lower levels of protein (**Figure 6**), similar to healthy controls. MCL-1 was not consistently overexpressed in primary CLL cells and levels differed between CLL patients and healthy donors (**Figure 6a**); however, no fold change could be assessed between the two groups (**Figure 6b**). These findings suggest that specific targeting of overexpressed BCL-2 by obatoclax in part relieves the inhibition to apoptosis.
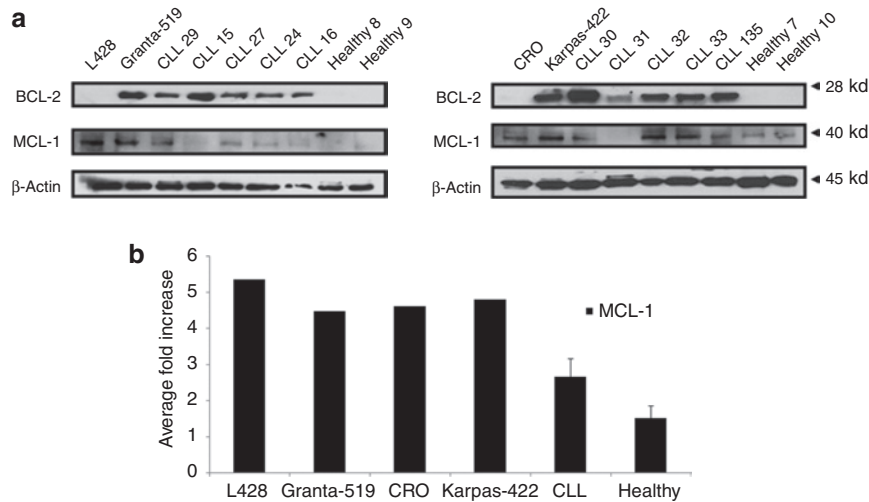

Figure 6 Expression of antiapoptotic BCL-2 family proteins. (**a**) Cells from four different B-lymphoma cell lines (L428, Granta-519, CRO, and Karpas-422), primary CLL cells and PBMCs from healthy donors were examined by immunoblotting for BCL-2 and MCL-1 expression. Protein lysate was isolated using 1% CHAPS buffer and BCL-2 and MCL-1 proteins were analyzed by western blot with anti-BCL-2 and MCL-1 antibodies. β-Actin was evaluated as a loading control. (**b**) The ratio of MCL-1 protein (black bars) in B-lymphoma lines and CLL patients ($n = 12$) was compared to MCL-1 levels in healthy volunteers ($n = 4$), respectively. Protein expression levels were quantified and normalized to β-actin level. The data shown are the mean ± SEM. BCL, B-cell lymphoma-2; CLL, chronic lymphocytic leukemia; PBMC, peripheral blood mononuclear cell; MCL-1, myeloid cell leukemia-1.

Combination treatment abrogates BCL-2/BAX and MCL-1/BAK interactions and promotes NOXA/BAX complexes

To examine interactions between pro- and antiapoptotic proteins following the VSV-obatoclax treatment, coimmunoprecipitation experiments were performed in Karpas-422 cells. MCL-1 and BAK interacted in nontreated cells (**Figure 7a**, lane 1) and this complex was only slightly disrupted with VSV or obatoclax (**Figure 7a**, lanes 2–3), but was insufficient to induce apoptosis
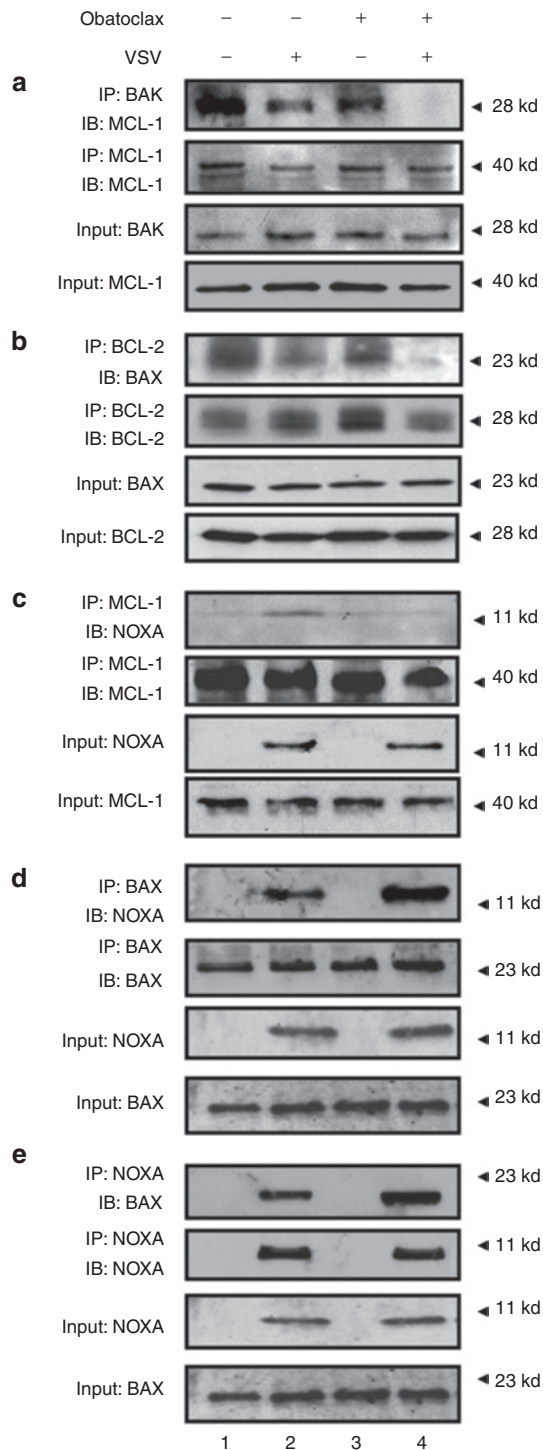
(**Figure 5a**, lane 3). VSV-obatoclax however caused complete loss of the MCL-1/BAK complexes (**Figure 7a**). Similarly, BCL-2 and BAX were constitutively present as a heterodimeric complex in untreated cells (**Figure 7b**, lane 1) and VSV or obatoclax alone had minimal effect on heterodimer formation (**Figure 7b**, lanes 2 and 3); clearly, the VSV-obatoclax combination caused almost complete dissociation of the BCL-2/BAX complex (**Figure 7b**, lane 4). In terms of NOXA-containing complexes, VSV-induced NOXA interacted with its cognate binding partner MCL-1 (**Figure 7c**, lane 2), whereas obatoclax alone or together with VSV disrupted NOXA/MCL-1 interactions (**Figure 8c**, lanes 3 and 4). The induction of NOXA, as well as the disruption of BCL-2–BAX interaction, suggested that NOXA and BAX may interact to form heterodimers. Coimmunoprecipitation with anti-BAX followed by immunoblot with anti-NOXA confirmed that NOXA interacted with BAX in VSV-infected cells (**Figure 7d**, lane 2) and VSV-obatoclax increased this interaction by three-fold (**Figure 7d**, lane 4). The reciprocal immunoprecipitation confirmed the identity of this novel NOXA-BAX heterodimer (**Figure 7e**). Altogether, these experiments argue that the VSV-obatoclax combination shifts the balance of BCL-2 family complexes toward those heterodimers that stimulate mitochondrial-dependent apoptosis in CLL cells.

DISCUSSION

The objective of the present study was to investigate the molecular mechanisms involved in VSV-obatoclax-mediated apoptotic synergism in CLL. We demonstrate: (i) enhanced cell killing in CLL cell lines, in primary CD5$^+$ CD19$^+$ CLL cells *ex vivo*, and in a murine model of lymphoma with the VSV-obatoclax combination; (ii) activation of the intrinsic apoptotic pathway, involving VSV-induced NOXA expression, BAX activation and translocation to the mitochondria and cytochrome C release; and (iii) mechanistically, disruption of BCL-2/BAX and MCL-1/BAK complexes and formation of proapoptotic complexes, including a novel NOXA/BAX heterodimer.

Figure 7 Combination treatment disrupts BCL-2/BAX and MCL-1/BAK interactions and promotes NOXA/BAX heterodimer formation. (**a**–**e**) Karpas-422 cells were treated with obatoclax (100 nmol/l) and VSV (10 MOI) for 24 hours. Protein lysates were prepared using 1% CHAPS buffer. (**a**) MCL-1 was immunoprecipitated (IP) from protein lysate and BAK interaction was revealed by immunoblotting using anti-BAK antibody. Protein inputs for BAK and MCL-1 are shown as separate bands at the bottom of the panel. (**b**) BCL-2 protein was immunoprecipitated with anti-BCL-2 antibody and coimmunoprecipitated proteins were detected using anti-BAX specific antibody. Protein inputs for BAX and BCL-2 are shown as separate bands at the bottom of the panel. (**c**) MCL-1 protein was immunoprecipitated with MCL-1 mAbs. MCL-1 immunoprecipitation was performed and bound fractions were analyzed by western blot for NOXA protein. Proteins inputs for NOXA and MCL-1 are shown as separate bands at the bottom of the panel. (**d**) BAX protein was immunoprecipitated, and coimmunoprecipitated NOXA protein was detected by western blot using a specific antibody for NOXA. Proteins inputs for NOXA and BAX are shown as separate bands at the bottom of the panel. (**e**) The reverse coimmunoprecipitation was performed in VSV- and obatoclax-treated cells. NOXA protein was immunoprecipitated with NOXA mAbs. Coimmunoprecipitated proteins were detected by immunoblot using specific antibody for BAX. Proteins inputs for NOXA and BAX are shown as separate bands at the bottom of the panel. BCL, B-cell lymphoma-2; mAb, monoclonal antibody; MCL, myeloid cell leukemia-1; MOI, multiplicity of infection; VSV, vesicular stomatitis virus.
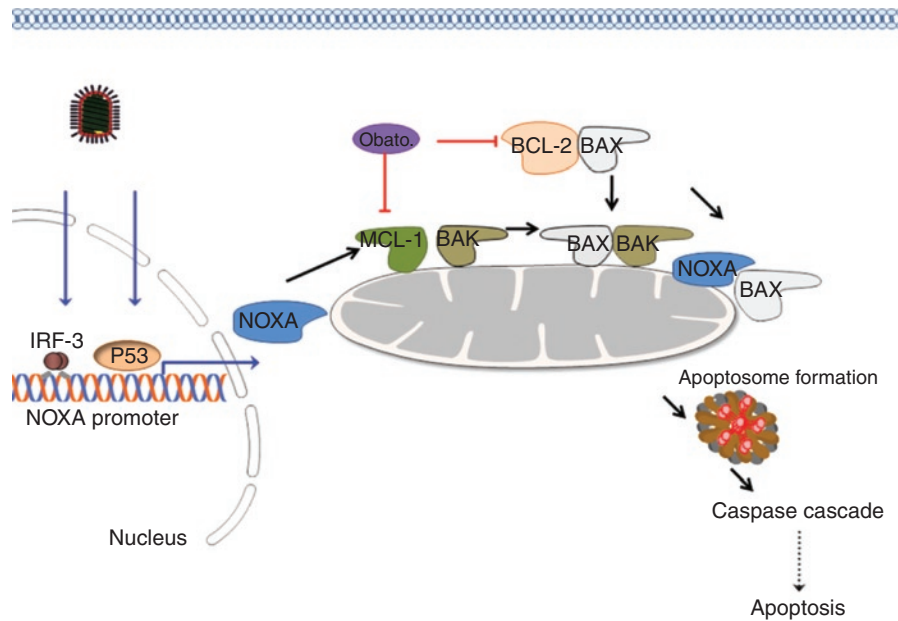
Figure 8 A proposed model of VSV-obatoclax synergism. In CLL cells, the proapoptotic activity of BAX and BAK are inhibited via association with antiapoptotic BCL-2 and MCL-1, respectively. obatoclax15-070 occupies the BH-3-binding groove of prosurvival BCL-2 and MCL-1 to disrupt BCL-2/BAX and MCL-1/BAK heterodimers, thus restoring the ability of the intrinsic apoptotic pathway to respond to VSV apoptotic stimuli. In response to VSV infection, the BH-3-only protein NOXA is induced at the transcriptional level, additionally contributing to the abrogation of MCL-1/BAK complexes. Activated NOXA protein may also directly induce a conformational change in BAX that subsequently promotes translocation to the mitochondria outer membrane. The VSV-obatoclax combination therapy leads to the activation and oligomerization of BAX and BAK homo- and heterodimers and thus membrane permeabilization, cytochrome c formation of the apoptosome and activation of the caspase cascade. BCL, B-cell lymphoma-2; CLL, chronic lymphocytic leukemia; MCL, myeloid cell leukemia-1; Obato., obatoclax; VSV, vesicular stomatitis virus.

There are several historical cases where patients with disseminated cancers have displayed improved conditions following viral vaccination.[33] Oncolytic virotherapy has emerged as an effective treatment for such cancers.[22,34] We and various groups have highlighted the ability of VSV to treat disseminated cancers such as CLL,[23] adult T-cell leukemia[25] and multiple myeloma[22] in preclinical models. Intravenous administration of the virus has been shown to be a successful method of therapy in various animal models and may translate well clinically for the treatment of CLL,[36,37] particularly at the stage where other treatments for advanced disease have failed. It is well understood that disseminated hematological malignancies will be difficult to treat and may require modified methods of therapy such as repetitive and carrier-cell based delivery of the virus.[34,38]

CLL is characterized by overexpression of antiapoptotic proteins such as BCL-2 and MCL-1.[3,4] BCL-2 overexpression is a hallmark of this disease and is found in most cases;[5] interestingly, high levels of MCL-1 expression strongly correlate with aggressive disease, negative clinical outcome and resistance to various treatments and is observed in ~30% of patients.[5–7] Under conditions where MCL-1 levels are high proapoptotic BAK can be sequestered by MCL-1 causing resistance to various therapies.[39,40] Although we identified BCL-2 overexpression in PBMCs from CLL patients and in Karpas-422 cells, MCL-1 levels on average were similar in CLL patients and healthy donors.

The effect of obatoclax on the disruption of MCL-1/BAK complexes has been characterized previously[21,39] but only one group investigated the effect of obatoclax on MCL-1/BAK interactions in CLL;[41] in this case, treatment was used in combination with

bortezomib, a proteasome inhibitor that leads to the accumulation of MCL-1 in CLL cells,[42] thus promoting MCL-1/BAK interaction and apoptotic resistance. Although MCL-1 overexpression was not observed in the CLL samples, Karpas-422 had elevated levels of MCL-1 and MCL-1/BAK complexes in resting cells. NOXA binds and inactivates MCL-1 protein, allowing the release and activation of BAK[40] and this interaction has been characterized in primary CLL following induction of NOXA.[39] Furthermore, NOXA induction has been observed in primary cells from CLL patients following treatment with histone deacetylase inhibitors[39] and aspirin[43] and was involved in regulating apoptosis and cell survival. The present study demonstrates that disruption of MCL-1/BAK complexes is the result of upregulation of NOXA by VSV and targeting of MCL-1 by obatoclax.

BH-3-only proteins are divisible into two groups: "sensitizers/depressors" that selectively bind antiapoptotic proteins, and "direct activators" that bind to antiapoptotic proteins and proapoptotic BAX and BAK.[8,44] Binding of "direct activators" BID and BIM to BAX and BAK has been shown to trigger conformational change and activation of BAX/BAK followed by mitochondrial outer membrane permeabilization.[8,45,46] NOXA is considered a "sensitizer/depressor" BH-3-only protein,[8,44] although a previous report suggested interaction between NOXA and BAX following double-stranded RNA or virus infection.[27] The present study is the first to identify endogenous NOXA-BAX heterodimers; NOXA is present at the mitochondria, as is activated BAX, suggesting that NOXA/BAX interactions at the mitochondrial surface contribute to membrane permeabilization, cytochrome c release, and apoptosis (**Figure 8**), Combination treatment is likely to affect

other BCL-2 family members; previous studies demonstrated that obatoclax can induce BIM expression and that inhibition of MCL-1 can alter the BAK activity, as well as BAX.[16,17,21] Additionally, other BCL-2 proteins may form apoptosis-inducing complexes that were not detected in the present study. Moreover, other groups have reported that activation of the JAK/STAT pathway can induce apoptosis in CLL cells.[47] Further studies will clarify the role of these additional proteins in VSV-obatoclax synergism.

Synergism between VSV and obatoclax appears to require three major events: NOXA upregulation, BAX release from BCL-2 and BAK release from MCL-1. The importance of NOXA in apoptotic induction[25–27] was highlighted by the observation that siRNA-mediated knockdown of NOXA decreased apoptosis in VSV-obatoclax treated cells and that VSV-mediated NOXA induction can be replaced with NOXA expression plasmids to synergistically induce apoptosis with obatoclax. VSV alone did not cause significant CLL cell death (**Figure 3a**, lanes 1–3), likely due to BAX sequestration by overexpressed BCL-2.[11] Although, NOXA induction by VSV was accompanied by a small increase in NOXA/MCL-1 interactions and a small decrease in MCL-1/BAK interactions, it was insufficient to shift the balance from prosurvival to proapoptotic complexes; only in combination with obatoclax did VSV completely relieve BCL-2 and MCL-1-mediated inhibition of BAX and BAK, respectively. These results strongly suggest NOXA expression is an important element in VSV-obatoclax-mediated cell death. In summary, we propose VSV-obatoclax therapy in primary CLL cells induces apoptosis via a mitochondrial-dependent pathway in which cytochrome c release and activation of caspases-9 and -3 are triggered by VSV-induced NOXA expression and obatoclax-induced release of BAX and BAK (**Figure 8**).

MATERIALS AND METHODS

Patients and PBMC isolation. PBMCs were obtained from healthy individuals and CLL patients at the Jewish General Hospital (Montreal, QC, Canada) following written informed consent, in agreement with the Jewish General Hospital and McGill University Research Ethics Committee. Patients had a median age of 60. Samples were collected from both male and female patients, although a majority were from male donors. The absolute lymphocyte counts were typical of CLL patients in general. Patients were not receiving treatment at the time of sample collection. PBMCs were isolated as previously described.[23] PBMCs were cultured in RPMI 1640 supplemented with 15% heat-inactivated fetal bovine serum (Wisent, St-Bruno, Quebec, Canada) and 100 U/ml penicillin–streptomycin. PBMCs were cultured at 37 °C in a humidified, 5% CO_2 incubator. CLL was confirmed by presence of $CD5^+$ and $CD19^+$ markers. Only patients with a 30% or greater $CD5^+/CD19^+$ CLL cell population were used in this study.[48,49]

Cell lines. The human B-lymphoma cell line Karpas-422 was purchased from the German Collection of Microorganisms and Cell Cultures (Braunschweig, Germany) and the A20 mouse B-lymphoma cell line was purchased from ATCC (Manassas, VA). All cell lines were grown in RPMI 1640 medium (Wisent, St Bruno, QC, Canada) supplemented with 10% fetal calf serum, penicillin and streptomycin. Cells were maintained at 37 °C and 5% CO_2.

Virus production, quantification, and infection. Construction of VSV-AV1 was previously described.[36] Virus stock was grown in Vero cells (purchased from ATCC, Bethesda, MD), concentrated from cell-free supernatants by centrifugation (15,000 r.p.m./4 °C/90 minutes) and titrated in duplicate by

standard plaque assay as previously described.[23] Primary PBMC isolates and Karpas-422 cells were infected with VSV at a multiplicity of infection of 10 plaque-forming units/cell for 1 hour in serum-free media at 37 °C. The cells were then incubated with complete medium at 37 °C for the indicated times.

Viability assay. Cell viability was assessed by 3-(4,5-dimethylthiazol)-2,5-diphenyl tetrazolium dye absorbance according to the manufacturer's instructions (Chemicon, Billerica, MA). PBMCs were seeded in 96-well plates at a density of 5×10^5 cells/well. Cell viability was also analyzed by Annexin V and propidium iodide staining and fluorescence-activated cell sorting analysis. For drug combination studies, cells were incubated with or without obatoclax (100 nmol/l) and infected or not with VSV-AV1 (10 multiplicity of infection) as indicated. To determine the IC_{50}, increasing concentrations of obatoclax (0–20 µmol/l) were used. Plates were incubated at 37 °C, 5% CO_2 and cells analyzed every 24 hours for 7 days. Each experimental condition was performed in quadruplicate.

Protein extraction and western blot analysis. Cells were washed twice with ice-cold phosphate-buffered saline, and proteins were extracted as described previously.[23] Briefly, cell pellets were lysed in ice-cold buffer containing phosphate-buffered saline, 0.05% NP40, 0.1% glycerol, 30 mmol/l NaF, 40 mmol/l β-glycerophosphate, 10 mmol/l Na3VO4, and protease inhibitor cocktail (Sigma-Aldrich, St Louis, MO) in 1/1,000 dilution. Extracts were kept on ice for 15 minutes and centrifuged at 10,000 g for 25 minutes (4 °C), and supernatants were stored at −80 °C. Protein concentration was determined with Bio-Rad protein assay reagent (BioRad, Hercules, CA). Protein extracts were resolved using 14% sodium dodecyl sulfate-polyacrylamide gel electrophoresis and transferred to nitrocellulose membrane (Hybond C Super; GE Healthcare Bio-Sciences, Buckinghamshire, UK). Membranes were blocked for 1 hour in 5% nonfat dried milk in TBST (Tris-buffered saline + 0.5% Tween-20). Followed by incubation with any of the following primary antibodies: cleaved caspase-3, β-actin, and BID (Cell Signaling Technologies, Danvers, MA; 1:2,000); BCL-2 (Santa Cruz Biotechnology, Santa Cruz, CA; 1:2,000), BAX (Santa Cruz Biotechnology; 1 µg/ml) and anti-mouse NOXA (Calbiochem, San Diego, CA; 1 µg/ml).

Mitochondria isolation. Mitochondria and cytosolic fractions were prepared from Karpas-422 cells after 24 hours of obatoclax and/or VSV-AV1 treatment, using the Pierce Mitochondria Isolation Kit for cultured cells, reagent-based method according with manufacturer protocol. Fractions were analyzed via western blot for cytochrome c (BD Biosciences, Franklin Lakes, NJ), BAX 6A7, BAX (Santa Cruz Biotechnology) and NOXA (Calbiochem). COXIV is an inner mitochondria membrane protein and was used as a measure of mitochondria purity and loading control; β-actin was used for cytoplasm purity and loading control.

Coimmunoprecipitation of BCL-2 family proteins. Two microgram of anti-BCL-2 monoclonal antibody, 2 µg of anti-BAX monoclonal antibody, 2 µg of anti-MCL-1 (Santa Cruz Biotechnology), 2 µg of anti-BAK monoclonal antibody (Millipore, Temecula, CA) or 2 µg of anti-NOXA monoclonal antibody (Calbiochem) were crosslinked to 20 µg of protein L-agarose beads (Santa Cruz Biotechnology) using 0.2 mol/l triethanloanime pH 8.0. Cells were lysed with 1% CHAPS lysis buffer [10 mmol/l HEPES (pH 7.4), 150 mmol/l NaCl, 1% CHAPS] containing protease inhibitors and total protein (500 µg) was incubated with crosslinked antibody in 1% CHAPS lysis buffer at 4 °C overnight on a rotator. Immunoprecipitates were collected by centrifugation for 1 minute. The pellets were washed three times with 1% CHAPS lysis buffer, beads were boiled in loading buffer and bound protein was analyzed by western blotting. Samples with antibody alone (no lysate), lysate alone (no antibody) or with an irrelevant isotype-matched immunoglobulin G antibody were used as negative controls (data not shown). Protein input (30 µg) was run in 14% sodium dodecyl sulfate-polyacrylamide gel electrophoresis and transferred to nitrocellulose

membrane (Hybond C Super; GE Healthcare Bio-Sciences). Membranes were blocked for 1 hour in 5% nonfat dried milk in TBST (Tris-buffered saline + 0.5% Tween-20) followed by incubation with any of the following primary antibodies: BCL-2, MCL-1 (Santa Cruz Biotechnology; 1:2,000), BAX (Sigma, St Louis, MO; 1 μg/ml), BAK (Millipore and NOXA (Calbiochem; 1 μg/ml).

RNA extraction and real-time PCR. Whole RNA from treated cells was extracted using RNase extraction Kit (Qiagen, Mississauga, ON, Canada) according to the manufacturer's instructions. Real time-PCR was performed using 1 μg and 200 ng (for Karpas-422 and *ex vivo* CLL cells, respectively) of RNA resuspended in RNase-free ddH$_2$O and Oligo dT12-18 primer (Invitrogen Canada, Burlington, ON, Canada) according to the manufacturer's conditions. Reverse transcription was performed using Superscript II (Invitrogen Canada) at 42 °C for 1 hour. The PCR primer pair specific for NOXA was: forward 5′-AGTAGCTGGAAGTCGAGTGT-3′ and reverse 5′-AGGTTCCTGAGCAGAAGAGT-3′. All data are presented as a relative quantification with efficiency correction based on the relative expression of target genes versus β-actin as reference gene. Complementary DNA was amplified using SyBR Green I PCR master mix (Applied Biosystems, Foster City, CA) and the data was collected using the AB 7500 Real-Time PCR System (Applied Biosystems) and analyzed by Comparative CT Method using the SDS v1.3.1 Relative Quantification Software. For semiquantitative real time-PCR, amplification products were resolved on an agarose gel and digital image of the ethidium bromide stained bands inverted for presentation.

In vivo *murine lymphoma model.* This study was approved by the local animal care and institutional animal ethics committee of Jewish General Hospital and McGill University. A total of eight animals were used for this study 4–6-week-old female Fox Chase SCID mice (Charles River Laboratories, Pointe Claire, QC, Canada) were injected subcutaneously with 1×10^6 A20 cells in a 100-μl volume into the hind flanks. Tumor volumes were measured and calculated as ½(length × width^2).[50] Once tumors were palpable, animals were randomly assigned to treatment groups and received five intraperitoneal injections of obatoclax (3 mg/day/kg). At days 2 and 5 following obatoclax injection, VSV-AV1 was inoculated intratumorally at 1×10^8 plaque-forming units of virus each. Animals were evaluated for signs of stress such as infection, dehydration, weight loss (>20%), and limb paralysis.

Transient transfection of siRNA NOXA and NOXA expression plasmid. Control and NOXA-specific RNAi sequences were described previously.[26] Transfection of Karpas-422 cells was carried out by electroporation using the Nucleofection System (Amaxa, Köln, Germany), according to the protocols proposed by the manufacturer. Briefly, 1×10^6 Karpas-422 cells were resuspended in 100 μl of nucleofector V solution (Nucleofector kit V) containing 100 pmol of double-stranded siRNAs. After electroporation (program T020), 500 μl of prewarmed cultured medium were added to the cuvette, and the cells were transferred into cultures plates containing prewarmed culture medium. At the optimal time of gene silencing (24 hours post-transfection), cells were mock-infected, treated or not with 100 nmol/l of obatoclax or infected with VSV 10 multiplicity of infection. After 24 hours cells were collected, protein was extracted, and immunoblots were performed.

Transfection of the pcDNA3-NOXA expression vector was carried out as described above with some changes. Briefly, 1×10^6 Karpas-422 cells were resuspended in 100 μl of nucleofector V solution (Nucleofector kit V) containing increasing amounts of pcDNA3-NOXA complemented with empty vector. Cells were treated with obatoclax 24 hours after transfection. Forty-eight hours post-transfection cells were collected, protein was extracted, and immunoblots were performed.

Statistical analysis. Graphics and statistical analysis were executed using GraphPad Prism 5 software (GraphPad Software, La Jolla, CA). Differences among the treatment groups were analyzed by paired *t*-test.

The *P* values <0.05 were considered statistically significant. Average values were expressed as mean ± SD.

REFERENCES
1. Caligaris-Cappio, F and Hamblin, TJ (1999). B-cell chronic lymphocytic leukemia: a bird of a different feather. *J Clin Oncol* **17**: 399–408.
2. Herishanu, Y and Polliack, A (2005). Chronic lymphocytic leukemia: a review of some new aspects of the biology, factors influencing prognosis and therapeutic options. *Transfus Apher Sci* **32**: 85–97.
3. Inamdar, KV and Bueso-Ramos, CE (2007). Pathology of chronic lymphocytic leukemia: an update. *Ann Diagn Pathol* **11**: 363–389.
4. Craig, RW (2002). MCL1 provides a window on the role of the BCL2 family in cell proliferation, differentiation and tumorigenesis. *Leukemia* **16**: 444–454.
5. Pepper, C, Lin, TT, Pratt, G, Hewamana, S, Brennan, P, Hiller, L *et al.* (2008). Mcl-1 expression has *in vitro* and *in vivo* significance in chronic lymphocytic leukemia and is associated with other poor prognostic markers. *Blood* **112**: 3807–3817.
6. Johnston, JB, Paul, JT, Neufeld, NJ, Haney, N, Kropp, DM, Hu, X *et al.* (2004). Role of myeloid cell factor-1 (Mcl-1) in chronic lymphocytic leukemia. *Leuk Lymphoma* **45**: 2017–2027.
7. Kitada, S, Andersen, J, Akar, S, Zapata, JM, Takayama, S, Krajewski, S *et al.* (1998). Expression of apoptosis-regulating proteins in chronic lymphocytic leukemia: correlations with *In vitro* and *In vivo* chemoresponses. *Blood* **91**: 3379–3389.
8. Chipuk, JE, Moldoveanu, T, Llambi, F, Parsons, MJ and Green, DR (2010). The BCL-2 family reunion. *Mol Cell* **37**: 299–310.
9. Kang, MH and Reynolds, CP (2009). Bcl-2 inhibitors: targeting mitochondrial apoptotic pathways in cancer therapy. *Clin Cancer Res* **15**: 1126–1132.
10. Brunelle, JK and Letai, A (2009). Control of mitochondrial apoptosis by the Bcl-2 family. *J Cell Sci* **122**(Pt 4): 437–441.
11. Willis, SN, Fletcher, JI, Kaufmann, T, van Delft, MF, Chen, L, Czabotar, PE *et al.* (2007). Apoptosis initiated when BH3 ligands engage multiple Bcl-2 homologs, not Bax or Bak. *Science* **315**: 856–859.
12. Vogler, M, Weber, K, Dinsdale, D, Schmitz, I, Schulze-Osthoff, K, Dyer, MJ *et al.* (2009). Different forms of cell death induced by putative BCL2 inhibitors. *Cell Death Differ* **16**: 1030–1039.
13. Campàs, C, Cosialls, AM, Barragán, M, Iglesias-Serret, D, Santidrián, AF, Coll-Mulet, L *et al.* (2006). Bcl-2 inhibitors induce apoptosis in chronic lymphocytic leukemia cells. *Exp Hematol* **34**: 1663–1669.
14. High, LM, Szymanska, B, Wilczynska-Kalak, U, Barber, N, O'Brien, R, Khaw, SL *et al.* (2010). The Bcl-2 homology domain 3 mimetic ABT-737 targets the apoptotic machinery in acute lymphoblastic leukemia resulting in synergistic *in vitro* and *in vivo* interactions with established drugs. *Mol Pharmacol* **77**: 483–494.
15. Mason, KD, Khaw, SL, Rayeroux, KC, Chew, E, Lee, EF, Fairlie, WD *et al.* (2009). The BH3 mimetic compound, ABT-737, synergizes with a range of cytotoxic chemotherapy agents in chronic lymphocytic leukemia. *Leukemia* **23**: 2034–2041.
16. Nguyen, M, Marcellus, RC, Roulston, A, Watson, M, Serfass, L, Murthy Madiraju, SR *et al.* (2007). Small molecule obatoclax (GX15-070) antagonizes MCL-1 and overcomes MCL-1-mediated resistance to apoptosis. *Proc Natl Acad Sci USA* **104**: 19512–19517.
17. Li, J, Viallet, J and Haura, EB (2008). A small molecule pan-Bcl-2 family inhibitor, GX15-070, induces apoptosis and enhances cisplatin-induced apoptosis in non-small cell lung cancer cells. *Cancer Chemother Pharmacol* **61**: 525–534.
18. Reed, JC and Pellecchia, M (2005). Apoptosis-based therapies for hematologic malignancies. *Blood* **106**: 408–418.
19. Trudel, S, Li, ZH, Rauw, J, Tiedemann, RE, Wen, XY and Stewart, AK (2007). Preclinical studies of the pan-Bcl inhibitor obatoclax (GX015-070) in multiple myeloma. *Blood* **109**: 5430–5438.
20. Witters, LM, Witkoski, A, Planas-Silva, MD, Berger, M, Viallet, J and Lipton, A (2007). Synergistic inhibition of breast cancer cell lines with a dual inhibitor of EGFR-HER-2/neu and a Bcl-2 inhibitor. *Oncol Rep* **17**: 465–469.
21. Pérez-Galán, P, Roué, G, Villamor, N, Campo, E and Colomer, D (2007). The BH3-mimetic GX15-070 synergizes with bortezomib in mantle cell lymphoma by enhancing Noxa-mediated activation of Bak. *Blood* **109**: 4441–4449.
22. Lichty, BD, Stojdl, DF, Taylor, RA, Miller, L, Frenkel, I, Atkins, H *et al.* (2004). Vesicular stomatitis virus: a potential therapeutic virus for the treatment of hematologic malignancy. *Hum Gene Ther* **15**: 821–831.
23. Tumilasci, VF, Olière, S, Nguyên, TL, Shamy, A, Bell, J and Hiscott, J (2008). Targeting the apoptotic pathway with BCL-2 inhibitors sensitizes primary chronic lymphocytic leukemia cells to vesicular stomatitis virus-induced oncolysis. *J Virol* **82**: 8487–8499.
24. Msaouel, P, Iankov, ID, Allen, C, Morris, JC, von Messling, V, Cattaneo, R *et al.* (2009). Engineered measles virus as a novel oncolytic therapy against prostate cancer. *Prostate* **69**: 82–91.
25. Goubau, D, Romieu-Mourez, R, Solis, M, Hernandez, E, Mesplède, T, Lin, R *et al.* (2009). Transcriptional re-programming of primary macrophages reveals distinct apoptotic and anti-tumoral functions of IRF-3 and IRF-7. *Eur J Immunol* **39**: 527–540.

26. Lallemand, C, Blanchard, B, Palmieri, M, Lebon, P, May, E and Tovey, MG (2007). Single-stranded RNA viruses inactivate the transcriptional activity of p53 but induce NOXA-dependent apoptosis via post-translational modifications of IRF-1, IRF-3 and CREB. *Oncogene* **26**: 328–338.
27. Sun, Y and Leaman, DW (2005). Involvement of Noxa in cellular apoptotic responses to interferon, double-stranded RNA, and virus infection. *J Biol Chem* **280**: 15561–15568.
28. Gaddy, DF and Lyles, DS (2007). Oncolytic vesicular stomatitis virus induces apoptosis via signaling through PKR, Fas, and Daxx. *J Virol* **81**: 2792–2804.
29. Gaddy, DF and Lyles, DS (2005). Vesicular stomatitis viruses expressing wild-type or mutant M proteins activate apoptosis through distinct pathways. *J Virol* **79**: 4170–4179.
30. Riedl, SJ and Shi, Y (2004). Molecular mechanisms of caspase regulation during apoptosis. *Nat Rev Mol Cell Biol* **5**: 897–907.
31. Billen, LP, Shamas-Din, A and Andrews, DW (2008). Bid: a Bax-like BH3 protein. *Oncogene* **27** Suppl 1: S93–104.
32. Riedl, SJ and Salvesen, GS (2007). The apoptosome: signalling platform of cell death. *Nat Rev Mol Cell Biol* **8**: 405–413.
33. Kelly, E and Russell, SJ (2007). History of oncolytic viruses: genesis to genetic engineering. *Mol Ther* **15**: 651–659.
34. Liu, C, Russell, SJ and Peng, KW (2010). Systemic therapy of disseminated myeloma in passively immunized mice using measles virus-infected cell carriers. *Mol Ther* **18**: 1155–1164.
35. Césaire, R, Olière, S, Sharif-Askari, E, Loignon, M, Lézin, A, Olindo, S *et al.* (2006). Oncolytic activity of vesicular stomatitis virus in primary adult T-cell leukemia. *Oncogene* **25**: 349–358.
36. Stojdl, DF, Lichty, BD, tenOever, BR, Paterson, JM, Power, AT, Knowles, S *et al.* (2003). VSV strains with defects in their ability to shutdown innate immunity are potent systemic anti-cancer agents. *Cancer Cell* **4**: 263–275.
37. Ebert, O, Harbaran, S, Shinozaki, K and Woo, SL (2005). Systemic therapy of experimental breast cancer metastases by mutant vesicular stomatitis virus in immune-competent mice. *Cancer Gene Ther* **12**: 350–358.
38. Power, AT, Wang, J, Falls, TJ, Paterson, JM, Parato, KA, Lichty, BD *et al.* (2007). Carrier cell-based delivery of an oncolytic virus circumvents antiviral immunity. *Mol Ther* **15**: 123–130.
39. Inoue, S, Riley, J, Gant, TW, Dyer, MJ and Cohen, GM (2007). Apoptosis induced by histone deacetylase inhibitors in leukemic cells is mediated by Bim and Noxa. *Leukemia* **21**: 1773–1782.
40. Gomez-Bougie, P, Wuillème-Toumi, S, Ménoret, E, Trichet, V, Robillard, N, Philippe, M *et al.* (2007). Noxa up-regulation and Mcl-1 cleavage are associated to apoptosis induction by bortezomib in multiple myeloma. *Cancer Res* **67**: 5418–5424.
41. Pérez-Galán, P, Roué, G, López-Guerra, M, Nguyen, M, Villamor, N, Montserrat, E *et al.* (2008). BCL-2 phosphorylation modulates sensitivity to the BH3 mimetic GX15-070 (Obatoclax) and reduces its synergistic interaction with bortezomib in chronic lymphocytic leukemia cells. *Leukemia* **22**: 1712–1720.
42. Nencioni, A, Hua, F, Dillon, CP, Yokoo, R, Scheiermann, C, Cardone, MH *et al.* (2005). Evidence for a protective role of Mcl-1 in proteasome inhibitor-induced apoptosis. *Blood* **105**: 3255–3262.
43. Iglesias-Serret, D, Piqué, M, Barragán, M, Cosialls, AM, Santidrián, AF, González-Gironès, DM *et al.* (2010). Aspirin induces apoptosis in human leukemia cells independently of NF-kappaB and MAPKs through alteration of the Mcl-1/Noxa balance. *Apoptosis* **15**: 219–229.
44. Kuwana, T, Bouchier-Hayes, L, Chipuk, JE, Bonzon, C, Sullivan, BA, Green, DR *et al.* (2005). BH3 domains of BH3-only proteins differentially regulate Bax-mediated mitochondrial membrane permeabilization both directly and indirectly. *Mol Cell* **17**: 525–535.
45. Lovell, JF, Billen, LP, Bindner, S, Shamas-Din, A, Fradin, C, Leber, B *et al.* (2008). Membrane binding by tBid initiates an ordered series of events culminating in membrane permeabilization by Bax. *Cell* **135**: 1074–1084.
46. Gavathiotis, E, Suzuki, M, Davis, ML, Pitter, K, Bird, GH, Katz, SG *et al.* (2008). BAX activation is initiated at a novel interaction site. *Nature* **455**: 1076–1081.
47. Liang, X, Moseman, EA, Farrar, MA, Bachanova, V, Weisdorf, DJ, Blazar, BR *et al.* (2010). Toll-like receptor 9 signaling by CpG-B oligodeoxynucleotides induces an apoptotic pathway in human chronic lymphocytic leukemia B cells. *Blood* **115**: 5041–5052.
48. Abbott, BL (2006). Chronic lymphocytic leukemia: recent advances in diagnosis and treatment. *Oncologist* **11**: 21–30.
49. Abbott, BL (2006). Recent advances in chronic lymphocytic leukemia. *Cancer Invest* **24**: 302–309.
50. Jensen, MM, Jørgensen, JT, Binderup, T and Kjaer, A (2008). Tumor volume in subcutaneous mouse xenografts measured by microCT is more accurate and reproducible than determined by 18F-FDG-microPET or external caliper. *BMC Med Imaging* **8**: 16.